ԵՐԵՎԱՆԻ ՊԵՏԱԿԱՆ ՀԱՄԱԼՍԱՐԱՆ

ՀԱՅԱՍՏԱՆԻ ՀԱՆՐԱՊԵՏՈՒԹՅԱՆ ԳԻՏՈՒԹՅՈՒՆՆԵՐԻ ԱԶԳԱՅԻՆ ԱԿԱԴԵՄԻԱ

ԿԻՍԱՀԱՂՈՐԴՉԱՅԻՆ ՄԻԿՐՈ- ԵՎ ՆԱՆՈԷԼԵԿՏՐՈՆԻԿԱ

ՏԱՍԵՐՈՐԴ ՄԻՋԱԶԳԱՅԻՆ ԳԻՏԱԺՈՂՈՎԻ ՆՅՈՒԹԵՐ
ԵՐԵՎԱՆ, 11-13 ՍԵՊՏԵՄԲԵՐԻ

SEMICONDUCTOR MICRO- AND NANOELECTRONICS

PROCEEDINGS OF THE TENTH INTERNATIONAL CONFERENCE
YEREVAN, ARMENIA, SEPTEMBER 11-13

ԵՐԵՎԱՆ 2015 YEREVAN

ՀՏԴ 620.3:544:06
ԳՄԴ 22.3+24.5
Կ 510

ICSMN-2015 ORGANIZING COMMITTEE

Vladimir Aroutiounian	***Conference Chairman***
	Yerevan State University, Armenia
Ferdinand Gasparyan	***Executive Secretary***
	Yerevan State University, Armenia
Edward Kazaryan	Russian-Armenian University, Armenia
Alexander Orlikovski	Physical-Technological Institute, Russia
Vazgen Melikyan	Synopsys, Armenia
Patrick Soukiassian	Paris-Sad/Orsay University, France
Martin Vrnata	Institute of Chemical Technology, Czech Republic
Azam Iraji Zad	Sharif University of Technology, IR Iran
Aram Vardanyan	"Barva" Innovation Center, Armenia
Ruben Vardanyan	State Engineering University of Armenia

Տպագրվում է Երևանի պետական համալսարանի ռադիոֆիզիկայի ֆակուլտետի գիտական խորհրդի որոշմամբ:

ԿԻՍԱՀԱՂՈՐԴՉԱՅԻՆ ՄԻԿՐՈ- ԵՎ ՆԱՆՈԷԼԵԿՏՐՈՆԻԿԱ: ՏԱՍԵՐՈՐԴ ՄԻՋԱԶԳԱՅԻՆ
Կ 510 ԳԻՏԱԺՈՂՈՎԻ ՆՅՈՒԹԵՐ ԵՐԵՎԱՆ, 11-13 ՍԵՊՏԵՄԲԵՐԻ.- Եր.: ԵՊՀ հրատ., 2015.- 180 էջ:

Ժողովածուի մեջ զետեղված են 2015 թ. սեպտեմբերի 11-13-ը Երևանում անցկացված «Կիսահաղորդչային միկրո- և նանոէլեկտրոնիկա» գիտաժողովում զեկուցված նյութերը: Աշխատանքները խմբավորված են ըստ հետևյալ բաժինների.

1. Նոր նյութեր և սարքեր.
2. Գազային և կենսաքիմիական սենսորներ
2. Նանոգիտություն և ցածր չափայնության համակարգեր.
3. Ինտեգրալ սխեմաների մշակում և մոդելավորում:

Ժողովածուն տպագրության է պատրաստվել փորձագիտական և խմբագրական հանձնախմբի կողմից:

ՀՏԴ 620.3: 544:06
ԳՄԴ 22.3+24.5

ISBN 978-5-8084-1991-9

SYNOPSYS BARVA

191,5 Million

Remember And Demand

The Conference Is Dedicated To

The 100th Anniversary Of The Armenian Genocide

Armenian scientists carry out intensive investigations in the field of physics and technology of semiconductors, semiconductor devices and nanotechnologies. New important results are obtained in micro- and nano-electronics. Many reports of Armenian scientists made in co-authorship with colleagues from several countries. Important results were obtained in Armenia in process of investigations of phenomena in sensors, photocells, transistors, large ICs, low-dimensional size effects, low-frequency noises peculiarities, and noise spectroscopy etc. It is evident that the geography of our Conference is expanded.

We hope that the Conference will go in a propitious and pleasant atmosphere, where new scientific ideas and foundations for novel projects.

The Organizing Committee whishes the participant's useful work, fruitful discussions, interesting polemics, genesis of new ideas and conceptions!

Thanks to State Committee of Sciences (of Ministry of Education and Science of the Republic of Armenia), "Barva" Innovation Center for the financial support and "Synopsys Armenia CJSC" for the contribution for awarding young scientists.

ORGANIZING COMMITTEE

September 1, 2015

Values of relaxation time, τ^*_2 for confined fluid can be obtained from Equations (7) and (8). The values of τ_1 and τ^*_2 thus obtained are used in Equation (9) to study the volume viscosity. Results obtained are shown in table 2 at two thermodynamic states represented by reduced temperatures and densities, i.e. for $T^* = 0.73$ and $n^* = 0.844$, $T^* = 1.83$ and $n^* = 0.500$ as a function of the width of the channel.

Table 2. Values of viscosity for different width of nano-channel (l). Viscosity is in units of 10^{-5} Pa s and *l* (in atomic diameter)

$T^* = 0.73$		$T^* = 1.83$	
l	η_b	l	η_b
5	11.05	5	2.86
10	8.23	10	1.47
15	5.84	15	1.25
20	5.34	20	1.1
30	5.1	30	1.08
40	5.08	40	1.05

Reduced temperature is defined as k_BT/e and reduced density $n\sigma^3$, where ε and σ are the parameters of LJ potential. It can be seen from table 2 that as we reduce width of nanochannel, the volume viscosity start increasing. For width of nanochannel up to 40σ (12 nm), the enhancement in viscosities is not significant. However, if width of channel is reduced further, viscosities start showing enhancement. It implies that for fluid confined to less than 10 nm, properties of fluids are different from that of bulk. Tendency of freezing is more in confined liquid as it is already having high viscosity. The behavior observed inconsistent with experimental/simulation observations of Zhang et al. [26], and can be attributed to the dynamical interaction between the fluid atoms and the wall.

References

1. ***P.J. Cadusch, B.D. Todd, J. Zhang, and P.J. Daivis.*** J. Phys. A: Math. Theor., v. 41, 035501(2008).
2. ***J. Mittal.*** J. Phys. Chem. B., v. 113 (42), 13800 (2009).
3. ***F. Sofos, T. Karakasidis, and A. Liakopoulos.*** Int. J. Heat Mass Transfer, v. 52, 735 (2009).
4. ***J.L. Xu and Z.Q. Zhou.*** Heat Mass Transfer, v. 40, 859 (2004).
5. ***Y.C. Liu, Q. Wang, T. Wu, and L. Zhang,*** J. Chem. Phys., v. 123, 234701 (2005).
6. ***A. Goyal, S. Sunita, and K. Tankeshwar.*** AIP Conf. Proc., v. 1393, 323 (2011).
7. ***E. Manontov, Yu.A. Kuntzerov, and S.B. Vakhrushev.*** Phys. Rev. E., v. 72, 051502 (2005).
8. ***R. Kaushal, S. Srivastava, and K. Tankeshwar.*** Int. J. Nanosci., v. 8, 543 (2009).
9. ***C. Sun, W.Q. Lu, B. Bai, and J. Liu.*** Int. J. Heat Mass Transfer, v. 55, 1732 (2012).
10. ***I. Bitsanis, T.K. Vanderlick, M. Tirell, and H.T. Davis.*** J. Chem. Phys., v. 89, 3152 (1988).
11. ***L. Bocquet and J.L. Barrat.*** Phys. Rev. Lett., v. 70, 2726 (1993).
12. ***S.C. Yang.*** Microfluid. Nanofluid, v. 2, 501 (2006).
13. ***T.M. Jeetain Mittal and J.R. Truskett.*** Phys. Rev. Lett., v. 100, 145901 (2008).
14. ***R. Devi, J. Sood, S. Srivastava, and K. Tankeshwar.*** Microfluid. Nanofluid, v. 9, 737 (2010).
15. ***F. Sofos, T.E. Karakasidis, and A. Linkopoulos.*** Int. J. Heat Mass Transfer, v. 53, 3839 (2010).
16. ***C. Zhang, Y. Chen, L. Yang, and M. Shi.*** Int. J. Heat Mass Transfer, v. 54, 4770 (2011).
17. ***Y. Wang, P. Keblinski, and Z. Chen.*** Phys. Rev. E., v. 86, 036313 (2012).
18. ***R. Qiao and N.R. Aluru.*** Langmuir, v. 21, 8972 (2005).
19. ***R.K. Sharma, K. Tankeshwar, K.N. Pathak, S. Ranganathan, and R.E. Johnson.*** Phys. Rev. E., v. 55 (2), 1550 (1997).
20. ***R.K. Sharma, K. Tankeshwar, and K.N. Pathak.*** J. Phys. Condense. Matter, v. 7, 537 (1994).
21. ***J.P. Hansen and I.R. MacDonald.*** Theory of Simple Liquids (Academic, New York, 1986).
22. ***K. Tankeshwar, B. Singh, and K.N. Pathak.*** J. Phys. Condense. Matter, v. 3, 3173 (1991).
23. ***K. Tankeshwar, K.N. Pathak, and S. Ranganathan.*** J. Phys. Condense. Matter, v. 8, 10847 (1996).
24. ***A.H.M. Zaheri, S. Srivastava, and K. Tankeshwar.*** Eur. Phys. J. B., v. 61, 465 (2008).
25. ***K. Tankeshwar and S. Srivastava.*** Nanotechnology, v. 18, 485714 (2007).
26. ***H. Zhang, B. Zhang, S. Liang, Y. Lu, W. Hu, and Z. Jin.*** Chem. Phys. Lett., v. 350, 247 (2001).
27. ***R. Kaushal and K. Tankeshwar.*** Phys. Rev. E., v. 68, 011201 (2003).

AHARONOV-BOHM OSCILLATIONS IN TYPE-II InAsSbP ELLIPSOIDAL QUANTUM DOTS

K.M. Gambaryan, V.G. Harutyunyan, V.M. Aroutiounian and L.S. Yeranyan

Yerevan State University, E-mail: kgambaryan@ysu.am

1. Introduction

Semiconductor quantum dots (QDs) confine electrons and holes in all three dimensions, which lead to a δ-like electronic density of states where the energy levels are totally quantized. This property is making them attractive for optoelectronic devices not only for improved laser diodes, but also for single photon sources, quantum computing systems and new generation QD-photodetectors [1]. For lasers less temperature sensitive threshold current and emission wavelength, as well as longer wavelengths to mid-infrared region can be achieved. This also leads to an increase in infrared photodetectors response and operating temperature as well as PV solar cells efficiency. For fundamental physics and technology, some phenomena such as the interaction between coupled dots, QD/nanopits cooperative structures, and the resolution of the quantum states in current-voltage and optoelectronic characteristics have been also observed [2-6]. Among quantum size objects' fabrication techniques, the self-organized Stranski–Krastanow (S–K) method is an important one by which dislocation-free nanostructures can be produced [7]. Depending on the growth conditions, the elastic strain can be relaxed by the formation of QDs, quantum rings or even unique island-pit pairs [1,3-6]. The energies of the conduction and valence band edges of InAs, InSb, InP and their ternary alloys exhibit highly interesting electronic properties of type-II nanostructures based on them. In particular, the band offsets of InSb in InAs suggest that electrons might be located in InAs (matrix), whereas the valence band maximum is inside InSb and thus makes this material a preferred option by the hole states [1,3-6]. Along with quantum rings, type-II QDs are particularly suitable for observing the Aharonov–Bohm effect (ABE) [8], since the constituent particles of the exciton, the electron and hole, are strongly polarized in radial direction due to the spatial separation of the carriers in such systems. In our InAsSbP type-II material system, the strong localization of hole within the QD, coupled with the Coulomb attraction to the otherwise free electron in the matrix defines the ring-like nature of the system. Specifically, in a magnetic field, the electron orbits the periphery of the QD with a phase proportional to the number of flux quanta (h/e) threading the area separating the electron in the InAs matrix from the strongly localized hole in the InAsSbP QD center. Oscillations in the photoluminescence intensity of quantum rings due to the optical ABE were first predicted by Govorov et al [9]. The first type-II system to display evidence of the optical ABE was InP/GaAs QDs [10], but here, the electron is strongly confined in the QD, while the hole resides in the GaAs matrix. Optoelectronic properties of InAs/GaAs QDs were investigated by magnetospectroscopic and magnetotransmission studies accompanied by PL measurements and Fourier-transform infrared spectrometry [11]. The optical ABE has been confirmed experimentally also in a number of II–VI type-II QDs [12].

In this paper, we describe the experimental evidence of magnetoresistance oscillations in InAsSbP composition type-II QDs grown on InAs(100) substrate. Using magnetospectroscopy, we have performed investigations, which were aimed at a general understanding of the unique physical nature and properties of grown QDs, as well as to identify possible ways to control their optoelectronic and magnetic behavior.

2. Experimental procedures and characterization techniques

The InAsSbP QDs under investigation were grown on InAs(100) substrate from a quaternary composition In-As-Sb-P melt by liquid phase epitaxy (LPE) with a modified slide-boat crucible using the S–K growth mode. QDs nucleation were performed at T=550°C constant temperature and contact duration of liquid phase with the substrate of 30 min. The diameter and height of liquid phase were equal to 8 mm and 150 μm, respectively. The industrial undoped n-InAs(100) ($n=2\cdot10^{18}$ cm^{-3} and 400 μm of thickness) was used as a substrate. According to the InAs–InSb–InP quasi-ternary phase diagram, concentrations of antimony and phosphorus in the quaternary growth solution were chosen to provide a lattice mismatch up to 1% between the InAs substrate and InAsSbP wetting layer at T=550°C. The atomic force microscope (AFM «Bruker Dimension Icon» with ScanAsyst) and «Keithley-6514 System Electrometer» were used for structural characterization and magnetospectroscopy. Mesa-chips in the form of PCCs were prepared for measurements. Lateral ohmic contacts to the samples were fabricated by the traditional thermal vacuum evaporation technique in the form of Cr/Au sandwich with further thermal annealing. The geometric configuration and topology of ohmic contacts were chosen to provide uniform lateral current flow and according to PCCs requirements. The sample's active surface was chosen to be equal to 10^{-2} cm^2.

3. Results and discussion

AFM images of QDs grown from In-As-Sb-P quaternary liquid phase on InAs(100) substrate are collected and presented in figure 1. Structural characterization shows that QDs are sufficiently uniformly distributed in large area (~1200 μm²) with an areal density ranging from 2 to 3×10⁸ cm⁻². AFM line-scan characterizations (Figs. 1(*b*,*c*)) show that the growth process and technological conditions result in an elongation of QDs in [010] direction with an average elongation ratio of 2.5:1.

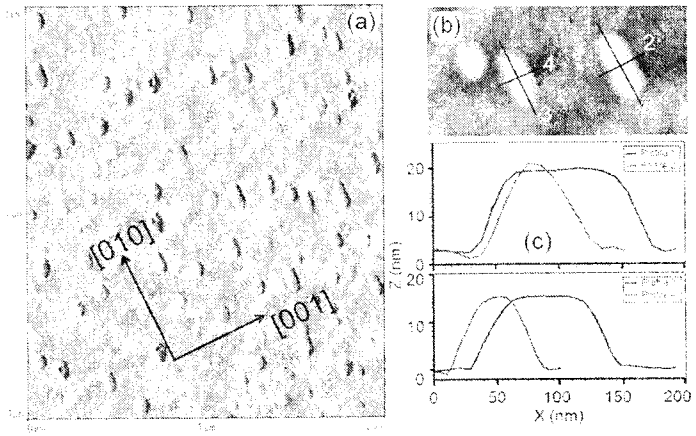

Fig. 1. AFM image (S=2×2 μm²) of QDs grown on InAs(100) substrate from In-As-Sb-P quaternary liquid phase – (*a*) AFM image with corresponding line scans – (*b*, *c*).

Magnetic field dependence of the electric sheet resistance (magnetoresistance) was measured in Faraday geometry at room and the liquid nitrogen temperatures. Measurements were performed at gradually increasing of the magnetic field up to 1 T with further decreasing up to zero. Magnetoresistance curves for our InAsSbP type-II QDs at room and T=78 K temperatures are presented in figures 2(*a*, *b*), respectively. Figure 2(*c*) shows the derivative of room temperature magnetoresistance curve measured at increasing magnetic field.

From Figs. 2(*a*–*c*) the periodic fractures on magnetoresistance curves, oscillations of the derivative curve with the period of $\delta B \approx 0.36 \div 0.38$ T, as well as the sheet resistance hysteresis of $\Delta R \sim 50$ mΩ ($\Delta B = 0.255$ T) and $\Delta R \sim 400$ mΩ ($\Delta B = 0.421$ T) at room and T=78 K temperatures, respectively, are glaring. Actually, type-II QDs and QRs are distinctly different from single or multiple stacked type-I QDs in that they have a not simply-connected geometry and that the charge carrier distribution is more complicated. For both cases, this geometry defines the ring-like trajectory for electrons (or holes) in magnetic field depending on band alignments. In our type-II QDs, for instance, holes are strongly localized inside the QDs, but the electron's wave function is "pushed" outside of the dot, as we have confirmed in previous calculations based on an eight-band **k·p**-simulation [3]. A schematic band structure in [001] direction and the model for an electron–hole pair in a type-II InAsSbP elongated QD in magnetic field is presented in figure 2(*d*). Evidently, the magnetic flux leads to a periodic change in the quantum mechanical properties of the encircling electrons. Therefore, upon the application of a magnetic field, the electron orbits the QD periphery producing an observable ABE. Rotation of the electron results in a periodic switching of the ground state with the angular momentum $l_z = 0$ to $l_z \neq 0$, in specific windows of magnetic field, as it is presented in Fig. 2(*c*).

However, in Fig. 2(*c*) four well-resolved oscillations with the period of $\delta B \approx 0.377$ T are evident. Since the period of oscillations should be approximately given by $\delta B = 4\Phi_0 / \pi D_e^2$ [12], where $\Phi_0 = h/e$ is the quantum flux, a diameter of $D_e \approx 120 \div 130$ nm is obtained. Calculated value for the electron's circling diameter is reasonable and coincides with the QDs optimal size in [010] direction (figure 1(*b*,*c*)). The selection rules for transitions in angular momentum are strictly valid only for the situation of perfect rotational symmetry and low temperatures (less than the temperature of thermal ionization of the exciton). Nevertheless, we assume that ABE oscillations are probable in our QDs system and that electrons perform the circular motion around the ellipsoidal QDs (Fig. 1(*b*)), since the substrate (matrix) is a high quality and undoped InAs crystal ($n \approx 2 \times 10^{16}$ cm⁻³; etch-pits density less than 10^4 cm⁻²), where the probability of electrons scattering on impurity or dislocation is negligibly small.

For magnetoresistance hysteresis, detected at both room and liquid nitrogen temperatures (figures 2(*a*, *b*)), using equation $\Delta E^{hyst} = \hbar \Delta B^{hyst} / 2\pi m^*$, we have evaluated numerical values of the remnant energy, which remain accumulated in the structure after switching off the magnetic field: $\Delta E^{hyst} = 1.04$ meV ($\Delta B = 0.255$ T at T=300 K) and $\Delta E^{hyst} = 1.71$ meV (for $\Delta B = 0.421$ T at T=78 K). Calculations were performed at $m^* = 0.028 m_0$ [6]. Evaluated energies explain and affirm experimental results described in our previous work [5]. We previously showed [5] that in the similar structure, the QDs are responsible for revealed additional peaks on the photoresponse spectrum (PR) at λ=3.56 μm and λ=3.65 μm and that even at very low applied voltages (*U* ≈ 1÷2 mV), a sufficient increasing of the PR signal on additional peaks occurred.

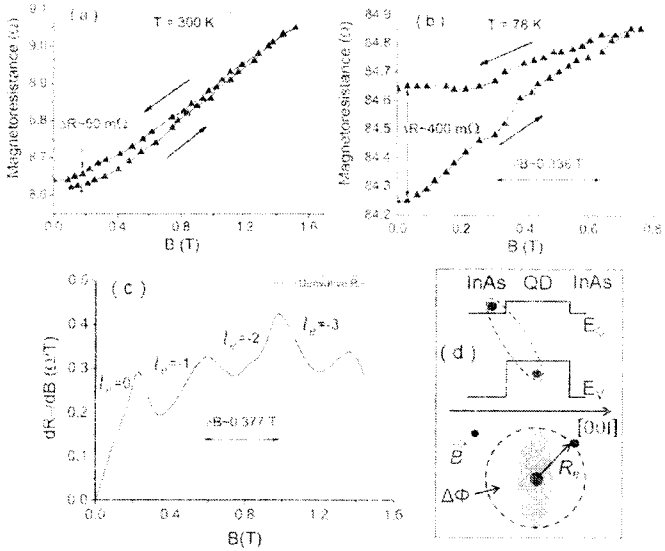

Fig. 2. Type-II QDs structure's sheet resistance versus magnetic field at Faraday (perpendicular to the substrate surface) geometry at room and liquid nitrogen temperature, respectively – (*a*, *b*); (*c*) – derivative of (*a*); (*d*) – schematic band structure in [001] direction and the model for an electron–hole pair in a type-II InAsSbP elongated QD.

4. Conclusions

Thus, the InAsSbP composition type-II QDs were grown on InAs(100) substrate. Aharonov-Bohm oscillations with the period of $\delta B \approx 0.38 \div 0.64$ T were found on the magnetoresistance curve at both room and liquid nitrogen temperatures. The magnetoresistance hysteresis equals to ~50 mΩ and ~400 mΩ was observed at room and liquid nitrogen temperature, respectively. Obtained experimental results have been explained by features typical to type-II QDs. Our study reveals a crucial influence of InAsSbP type-II QDs on magnetic and other properties of device structures based on InAs crystals, in particular photoconductive cells and other mid- and far-infrared devices.

References

1. *D. Bimberg, M. Grundmann and N.N. Ledentsov.* Quantum Dot Heterostructures. Wiley, New York, 1998.
2. *P. Bhattacharya, X.H. Su, S. Chakrabarti, G. Ariyawansa and A.G.U. Perera.* Appl. Phys. Lett., v. 86, 191106 (2005).
3. *O. Marquardt, T. Hickel, J. Neugebauer, K.M. Gambaryan and V.M. Aroutiounian.* J. Appl. Phys., v. 110, 043708 (2011).
4. *K.M. Gambaryan.* Nanoscale Res. Lett., v. 5, 587 (2010).
5. *K.M. Gambaryan, V.M. Aroutiounian and V.G. Harutyunyan.* Infrared Phys. & Tech., v. 54, 114 (2011).
6. *K.M. Gambaryan et al.* Appl. Phys. Lett., v. 100, 033104 (2012).
7. *I. Stranski and L. Krastanow.* Math.-Naturwiss., v. 146, 797 (1938).
8. *Y. Aharonov and D. Bohm.* Phys. Rev., v. 115, 485 (1959).
9. *A.O. Govorov, S.E. Ulloa, K. Karrai and R.J. Warburton.* Phys. Rev. B, v. 66, 081309(R) (2002).
10. *I. Ribeiro, A.O. Goverov, W. Carvalho, Jr. and G. Medeiros-Ribeiro.* Phys. Rev. Lett., v. 92, 126402 (2004).
11. *V. Preisler, R. Ferreira, S. Hameau et al.* Phys. Rev. B, v. 72, 115309 (2005).
12. *V.M. Fomin.* Physics of Quantum Rings. Springer-Verlag, Berlin, 2014.